

Synthesis and Characterization of Cerium Oxide Nanoparticles using Sucrose as a Green Capping Agent and its application for Antibacterial and Humidity Sensor Studies

A.Mobeen and R. Sundaram*

PG and Research Department of Chemistry, Presidency College (Autonomous), Chennai 600 005, Tamil Nadu, India.

**Corresponding author: drsundarampresidency@gmail.com*

Abstract -Cerium oxide nanoparticles (CeO₂ NPs) were prepared by co-precipitation method using cerium chloride and sodium hydroxide (NaOH) in presence of sucrose as a green capping agent. The obtained yellowish white powder was characterized via X-ray diffraction studies (XRD), transmission electron microscopy (TEM), Fourier transform infrared spectroscopy (FT-IR), X-ray energy dispersive spectroscopy (EDX), UV-Visible spectroscopy and photoluminescence (PL). The antibacterial activity of the synthesized nanoparticles were observed in two Gram-negative and one Gram-positive bacterial pathogens, which exhibits encouraging result and shows the zone of inhibition increased with concentration of the nanoparticles. The sensor measurement was carried out by observing linear decrease in dc resistance with relative humidity at different humidity environment (RH_{5%} to RH_{98%}). The response and recovery time and the sensitivity factor $S_f = 2876$ was calculated. The results illustrates that the synthesized cerium oxide nanoparticles acts a good sensor element to apply in humidity sensor and antibacterial applications.

Key words: Antibacterial activity, Cerium oxide nanoparticles, Green capping agent, Humidity measurement

1. INTRODUCTION

Cerium oxide or ceria (CeO₂) is a lanthanide rare earth metal oxide having face centred cubic (FCC) fluorite type structure [1]. Nanoceria exists a cycle between the Ce³⁺ and Ce⁴⁺ valence states and it acts as a regenerative catalyst owed to the presence of oxygen vacancies [2]. In recent years the synthesis of nanoceria become more attention due to its outstanding properties such as large band gap energy (3.19eV), chemical stability, high thermal stability and dielectric properties ($\epsilon=24.5$) [3]. These properties of CeO₂ enhance in wide spread of application like waste water treatment, bio-sensors, corrosion protection, photo catalytic efficiency, cosmetics and pharmaceuticals[1,4-8] Currently researchers focused on the antibacterial activity of cerium oxide nanoparticles (CeO₂ NPs) because of its excellent redox nature also it hinder the bacterial growth and scavenging free radicals [9]. Furthermore the non-aggregated NPs are very important to use in practical application, to achieve this expectation researchers will focused to reduce the aggregation of NPs during preparation process. In generally surfactants or capping agents are used

to control the aggregation and agglomeration of metal oxides. In the case of CeO₂ NPs it is very difficult to control the aggregation because of its high surface energy and activity [10]. Fatemeh Sadat et.al reported that the agglomeration of nanoparticles were reduced using carbohydrate sugars as a capping agent [11]. From the literature study we decided to use sucrose as a green capping agent as it is eco-friendly, non-toxic, low cost and easily available.To the best of our knowledge no research work was done using sucrose as a capping agent for the preparation of CeO₂ NPs by co-precipitation method. The foremost objective of this study is to find the structure, morphology, optical, humidity sensor and anti-bacterial studies of the synthesized CeO₂ NPs.

2. MATERIALS AND METHODS

The chemicals used to prepare CeO₂ NPs were analytical grade and used without further purification. Cerium ammonium nitrate Ce(NH₄)₂(NO₃)₆, Sodium hydroxide NaOH, Sucrose, Ethanol and deionised water used for all experiments.

2.1 Preparation of the sample

In a typical procedure 0.1M of $Ce(NH_4)_2(NO_3)_6$ solution was added to 0.1M of Sucrose solution. 0.03 M of NaOH was added drop wise to the above solution with constant stirring to reach PH=11. The clear solution turned yellowish after the reaction it was converted into light yellowish suspension. Thereafter the reaction continued for further 3 hrs under magnetic stirring at room temperature. The final precipitate was washed several times with deionised water followed by ethanol. It was filtered and dried at $100^{\circ}C$ for 4hrs to obtain pure CeO_2 NPs, finally the powder was calcined at $500^{\circ}C$ for 3hrs.

2.2 Characterization

The prepared CeO_2 NPs sample was characterized by the following techniques. The phase purity and crystallite size of the particles were analysed via Powder X-ray diffraction studies (XRD). The morphology and microstructure of CeO_2 NPs were confirmed by SEM and TEM techniques. The optical properties and functional group identification was done through UV-vis, PL emission and FTIR spectroscopy respectively.

2.3 Humidity sensor measurement

The method was followed as we mentioned in our earlier published work in Elsevier [12]. The controlled humidity was attained in different humidity environments such as anhydrous (5%) P_2O_5 , (20%) CH_3COOK , (31%) $CaCl_2 \cdot 6H_2O$, (42%) $Zn(NO_3)_2 \cdot 6H_2O$, (51%) $NaNO_2$, (66%) NH_4Cl , (79%) $BaCl_2 \cdot 2H_2O$ and (98%) $CuSO_4 \cdot 5H_2O$. The sensor element prepared with a fabricated pellet (10mm diameter and 1 mm thickness) consist of copper wire on both sides, the powder sample was dissolved in ethanol then dispensed on the pellet which dried at room temperature, finally it was kept at the above humidity environments to measure the sensitivity of the sample. The variation of dc resistance with relative humidity (RH 5-98%) was measured with the help of barigo hygrometer.

2.4 Antibacterial assay

The antibacterial activity of the CeO_2 NPs was examined by agar well diffusion method against three bacterial pathogens *Staphylococcus aureus*, *Escherichia coli* and *Pseudomonas aeruginosa* at different concentration of the samples. The stock bacterial culture was stored at 4

$^{\circ}C$, the active culture was prepared by transferring a loop of stock culture to the nutrient broth which was incubated at $37^{\circ}C$ for 24 hrs and the turbidity was adjusted to Man Farland 0.5. Muller- Hinton agar was poured into the petriplates aseptically it was allowed to solidify, the lawns were made by sterile cotton and the wells were cuts with the help of sterile cork borer. The sample extract at different concentration 1.56, 3.125, 6.25, 12.5, 25 and 50 mg/ml was poured into the wells, finally the plates were incubated aerobically at $37^{\circ}C$ for 24 hrs. Afterward the antibacterial activity was estimated by measuring the inhibition zone formed around the well.

3. RESULTS AND DISCUSSION

3.1 XRD studies

The phase identification and crystalline size of as synthesized cerium oxide nanoparticles (CeO_2 NPs) were characterized by Powder X-ray diffraction pattern as shown in Fig.1. It reveals the four diffraction peaks correspond to the cubic phase of CeO_2 at 2θ angle = 29.10° (111), 31.46° (200), 48.95° (220) and 54.68° (311) respectively. All the diffraction peaks were indexed to cubic phase of CeO_2 having cell parameter $a=5.411 \text{ \AA}$ belong to $Fm\bar{3}m$ space group and also well matched with (JCPDS Card No: 34-394). The crystallite size of the sample was calculated using Scherrer's equation:

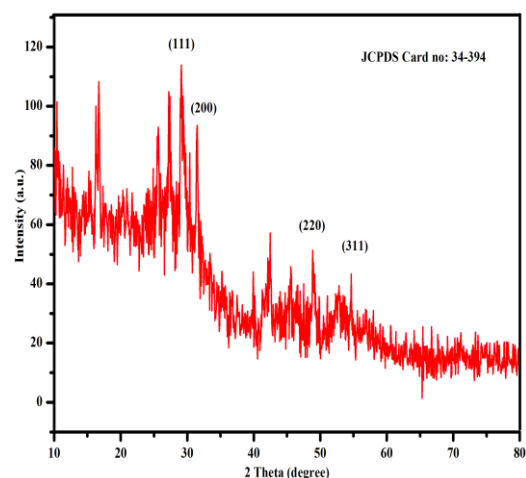


Fig.1. Powder XRD analysis of as synthesized CeO_2 NPs.

$$D=0\lambda/\beta hkl \cos\theta$$

Where D is the crystallite size, β is the full width half maximum (FWHM), θ is the diffraction angle and λ is the wavelength of the incident X-ray. The calculated crystallite size of sample was 29.05 nm for the most predominant peak at $2\theta = 29.10^\circ$ (111) with d space value of 3.068 \AA . The development of the sharp peaks in the spectrum suggested the good crystallinity of the CeO_2 NPs.

3.2 FTIR spectroscopy

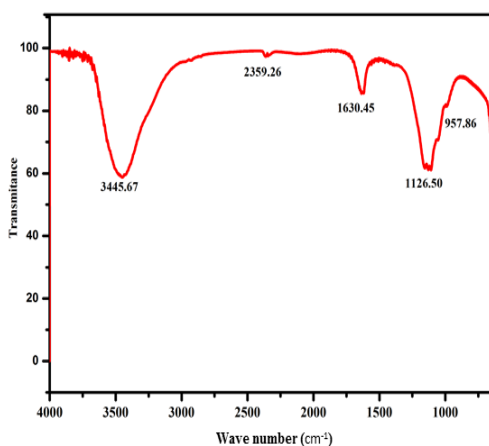


Fig.2. FTIR Spectrum of as synthesized CeO_2 NPs.

The bonding nature and the presence groups were observed through FT-IR spectrum as shown in Fig.2. In this spectrum, the absorption bands appeared at 957, 1126, 1630, 2359 and 3445 cm^{-1} , established the existence of pure CeO_2 phase. Additionally the bands below 1000 cm^{-1} is ascribed to stretching vibration of Ce-O [13]. The band located at the region of 1630 and 3445 cm^{-1} are assigned to bending and stretching vibrations of –OH group present on the surface of CeO_2 NPs. The bands near 1126 cm^{-1} is attributed to the presence of C-O-H group, which confirms the electrostatic force between sucrose chains and CeO_2 NPs.

3.3 Morphological studies

The surface morphology and size of the CeO_2 NPs were examined by Scanning electron microscopy (SEM). Fig.3 shows the bunches of small spherical particles at different magnification and it clearly displays that the agglomeration of the CeO_2 NPs was reduced by green capping agent used in the preparation process, however the images specifies high porosity on the surface of the CeO_2 NPs which enhances the sensitivity of the sample.

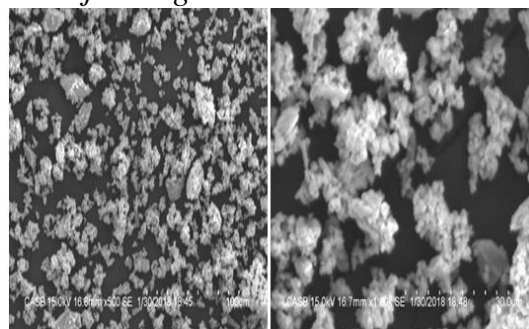


Fig.3. SEM images of CeO_2 NPs.

Further, the microstructure and size of the CeO_2 NPs was determined by TEM technique. Fig.4 reveals the corresponding selected area electron diffraction pattern (SAED) of the sample at 0.01 nm, it exhibits the diffraction ring of cubic fluorite structure and the spots indicates the high degree of crystallinity of CeO_2 NPs [14]. The bright spots confirms the formation of plane (111) with d space value of 3.068 \AA , In addition it is well matched with XRD and SEM results.

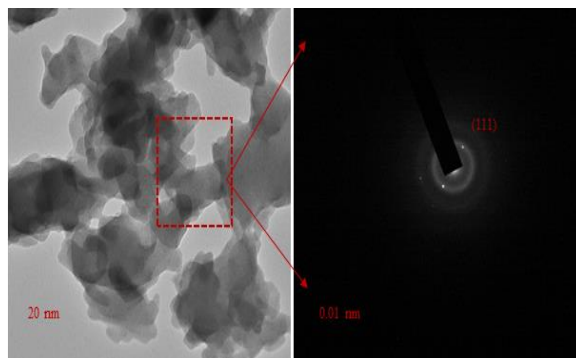


Fig.4. TEM images of CeO_2 NPs

3.4 Optical studies

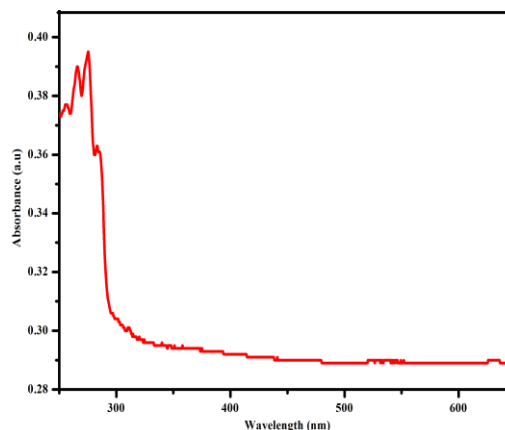


Fig.5a UV-vis absorption spectroscopy

Fig.5a displays the UV-visible spectroscopy and it exhibits the absorption peak at 283.76 nm. It shows better optical property, whereas the presence of the peak at 283.76 nm relates the quantum size effect of blue shift and confirms the charge transition takes place between the O 2p and Ce 4f states in O²⁻ and Ce⁴⁺ [15,16]. The band gap energy of the particles was calculated using Tauc's equation shown in Fig 5b.

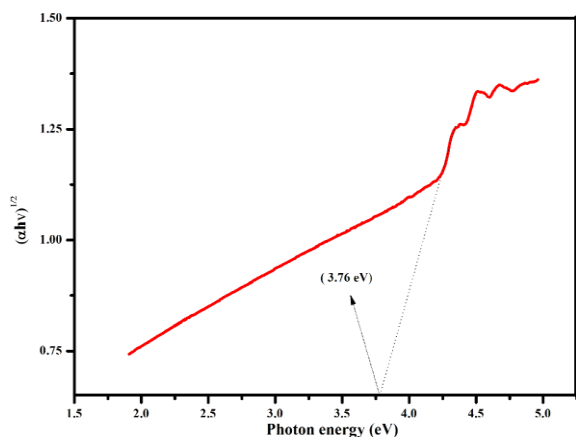


Fig.5b. Band energy plot of CeO₂ NPs by Tauc's equation.

The extrapolation of straight line on energy axis (hv) will give direct band gap and it was found to be 3.76 eV, which is well contest with reported value 3.78eV for Cerium oxide [17] and it is higher band gap value than bulk CeO₂ (3.19 eV).

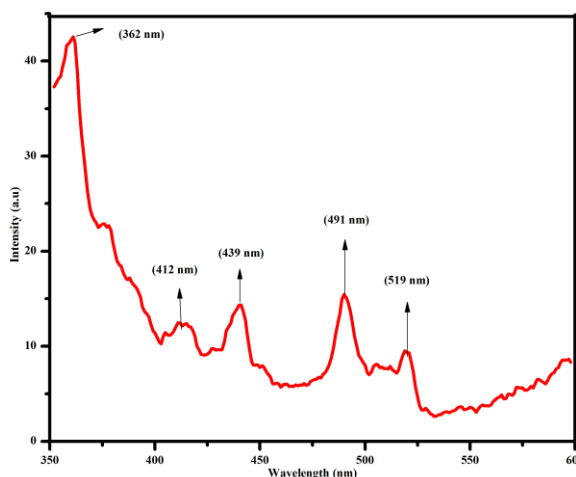


Fig. 6. displays photoluminescence spectra of CeO₂ NPs.

Fig.6 shows the PL emission spectra of CeO₂ NPs excited at 350 nm and the spectrum displays multiple emission peak. The weak UV emission peak centered at the region of 362 nm is

corresponds to band edge emission, a weak blue emissions peak at 412 nm is ascribed to the presence of surface defects. The blue emission peak centered at 439 nm is assigned to high level transition in CeO₂ NPs. The weak blue-green emission peak at 491 nm can be attributed to the formation of oxygen vacancies during the preparation of the sample. Finally the broad green emission peak centered at 519 nm is due to the radiative recombination of excitations and the surface defects are existing between Ce the inner 4f-5d transition and O 2p valence state [18].

3.5 Antibacterial studies

The antibacterial activity of CeO₂ NPs was done in three bacterial species *staphylococcus aureus*, *pseudomonuas aeruginosa* and *Escherichia coli* by Agar well diffusion method under six different concentration of the sample as shown in Fig.7a.

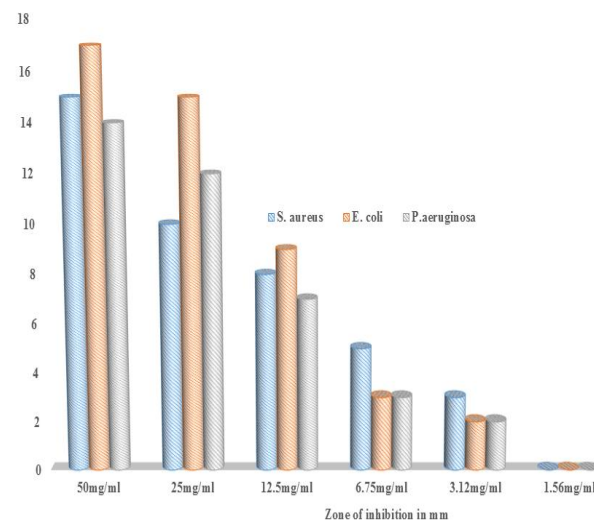


Fig.7a Diameter of the zone of inhibition of the micro-organism at different concentration of CeO₂ NPs.

The results shows that the CeO₂ NPs possess higher antibacterial activity against *Escherichia coli* compared to the other two bacterial pathegons. At high concentration 50 mg/ml *Escherichia coli* possess higher (17 mm) zone of inhibition, however it is observed low in *pseudomonuas aeruginosa*. All the bacterial pathegons didn't show activity at lower concentration 1.56 mg/ml of the sample. Table.1 shows that the zone of inhibition was increased with sample concentration.

Infact the larger surface area of the nanoparticles enhance the oxygen vacancies, passage of highly reactive molecules due to

porosity. The good crystalline nature of the sample enhance the formation of reactive oxygen species [19]. In our studies the positively charged CeO₂ NPs react with negatively charged cell membrane of given bacteria owing to electrostatic interaction finally it leads to bacterial death [20]. Also the diameter of zone of inhibition of bacterial species was observed in the order of *Escherichia coli* > *pseudomonas aeruginosa* > *pseudomonas aeruginosa*.

3.6 Humidity sensor studies

Fig.8a shows the change in resistance log R with relative humidity RH % of CeO₂ NPs measured at room temperature. Humidity sensor operating at room temperature having the advantage of protonic conduction on the surface of the semi-conduction materials. The presence of high porosity nature on the surface of CeO₂ NPs

The plot of log R vs RH% shows a linear curve, also decrease in resistance at 5-98% of RH for CeO₂ NPs. The sensitivity factor S_f was calculated by R_{5%}/R_{98%}, where R_{5%} and R_{98%}, are dc resistance at RH 5% and RH 98%. The calculated S_f value was found to be S_f = 2876, however the higher value of S_f raise the sensitivity of sample towards a moisture [22]. The response and recovery time was studied and the graph of log R vs Time was measured for RH 5% and RH 98% as shown in Fig.8b. The response and recovery time was found to be 45s and 197s respectively. The observed results conclude that the stability of CeO₂ NPs is appreciable to utilise in sensor applications.

Table.1 Diameter of Zone of inhibition in mm

Micro-organism	Zone of inhibition in mm					
	50mg/ml	25mg/ml	12.5mg/ml	6.75mg/ml	3.12mg/ml	1.56mg/ml
<i>Staphylococcus aureus</i>	15	10	8	5	3	Nil
<i>Escherichia coli</i>	17	15	9	3	2	Nil
<i>Pseudomonas aeruginosa</i>	14	12	7	3	2	Nil

Nil = No antibacterial activity.

encourage the change in resistance with relative humidity level due to adsorption and capillary condensation [21].

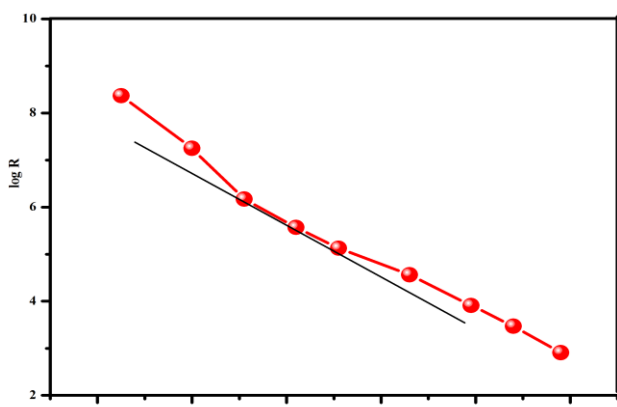


Fig.8a. Humidity sensor measurement, a plot of log R Vs RH.

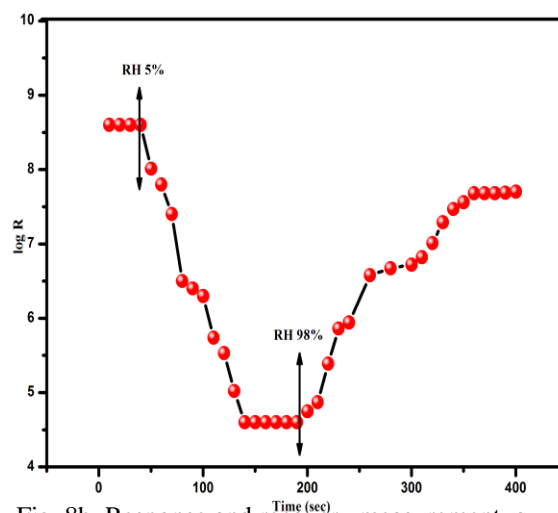


Fig. 8b. Response and recovery measurement, a plot of log R Vs Time (sec).

4. CONCLUSION

We conclude that the samples were successfully prepared by simple co-precipitation method. The XRD pattern determined the formation of cubic phase of CeO₂ with crystallite size of 29.05 nm. The CeO₂ NPs exhibits bunches of small spherical like morphology with high porosity. The samples exhibits the multiple emission peaks centred at 362,412,439,491 and 519 nm and the calculated band gap 3.76 eV. The humidity sensing measurement illustrates CeO₂ NPs highest sensitivity factor $S_f = 2876$ with response time of 45s and recovery time of 197s respectively. The antibacterial studies of CeO₂ NPs reveals encouraging antibacterial activity against both Gram- positive and Gram-negative bacteria.

Acknowledgement

This research work is supported by Maulana Azad National Fellowship (MANF), UGC-MHRD, Govt. of India, and New Delhi through SRF grant No.F.17.1/2016/MANF-2015-17-TAM-62835/ (SA-III/website).

I am very much thankful to Dr. SK. Jasmine Shahina, Asst.Prof and Summera Rafiq, Associate Prof & HOD, Dept. of Microbiology, JBAS College for Women (Autonomous), Teynampet, Chennai-18. For extending the Lab facilities to do antibacterial studies.

REFERENCES

- [1] S. K. Kannan and M. Sundrarajan, "A Green Approach for the synthesis of a Cerium Oxide Nanoparticle: Characterization and Antibacterial Activity", *International Journal of Nanoscience*, Vol. 13(3), pp. 1450018, 2014.
- [2] E. G. Heckert, A. S. Karakoti, S. Seal and W. T. Self, "The role of cerium redox state in the SOD mimetic activity of nanoceria", *Biomaterials*, Vol. 29 (18), pp. 2705-2709, 2008.
- [3] J. J. Miao, H. Wang, Y. R. Li, J. M. Zhu and J. J. Zhu, "Ultrasonic induced synthesis of CeO₂ nanotubes", *J.Cryst. Growth*, Vol. 281, pp. 525-529, 2005.
- [4] S. Thakur and P. Patil, "Rapid synthesis of cerium oxide nanoparticles with superior humidity- sensing performance", *Sens. Actuator B*, Vol. 194, pp. 260-268, 2014.
- [5] Y. Xingwen, C. Chunan, Y. Zhiming, Z. Derui and Y. Zhungda, *Corrosion Science*, Vol. 43, pp. 1283-1294, 2001.
- [6] B.Li, T. Gu, T. Ming, J. Wang, P. Wang and J. C. Yu, "Gold Core @ Ceria Shell nanostructures for plasmon-enhanced catalytic creations under visible light", *ACS Nano*, Vol. 8, pp. 8152-8162, 2014.
- [7] Toshiyuki Masui, Hidekazu Hirai, Ryo Hamada, Nobuhito Imanaka, Gin-ya Adachi, Takao Sakatac and Hirotarō Moric, "Synthesis and characterization of cerium oxide nanoparticles coated with turbostratic boron nitride", *J. Mater. Chem*, Vol. 13, pp. 622-627, 2003.
- [8] A. Thill, O. Zeyons, O. Spalla, F. Chauvat, J. Rose, M. Auffan and A. M. Flank, "Cytotoxicity of CeO₂ nanoparticles for Escherichia coli. Physico-chemical insight of the cytotoxicity mechanism", *Environ. Sci. Technol*, Vol. 40, pp. 6151-6156, 2006.
- [9] S. Babu, A. Velez, K. Wozniak, J. Szydłowska and S. Seal, "Electron paramagnetic study on radical scavenging properties of ceria nanoparticles", *Chem Phys Lett*, Vol. 442, pp. 405-408, 2007.
- [10] Kang-Qiang Liu, Cheng-Xiu Kuang, Ming-Qiang Zhong, Yan-Qin Shi and Feng Chen, "Synthesis, characterization and UV-shielding property of polystyrene-embedded CeO₂ nanoparticles", *Optical Materials*, Vol. 35, pp.2710-2715, 2013.
- [11] Fatemeh Sadat Sangsefidi, Majid Nejati, Javad Verdi and Masoud Salavati-Niasari, "Green synthesis and characterization of cerium oxide nanostructures in the presence carbohydrate sugars as a capping agent and investigation of their cytotoxicity on the mesenchymal stem cell", *Journal of Cleaner Production*, Vol. 156, pp. 741-749, 2017.
- [12] A. Mobeen Amanulla, SK. Jasmine Shahina, R. Sundaram, C. Maria Magdalane, K. Kaviyarasu, Douglas Letsholathebe, S. B. Mohamed, J. Kennedy and M. Maaza, "Antibacterial, magnetic, optical and humidity sensor studies of β -CoMoO₄-Co₃O₄ nanocomposites and its synthesis and characterization", *Journal of Photochemistry B: Biology*, Vol. 183, pp. 233-241, 2018.
- [13] M. K. Amosa, "Process optimization of Mn and H₂S removals from POME using an enhanced empty fruit bunch (EFB) - based adsorbent produced by pyrolysis", *Environ. Nanotechnol. Monit. Manage*, Vol. 4, pp. 93-105, 2015.
- [14] S. Phoka, P. Laokul, E. Swatsitang, S. Promarak and Maensiri, *Mater. Chem. Phys*, Vol. 115, pp. 423-428, 2009.
- [15] S. B. Khan, M. Faisal, M. M. Rahman and A. Jamal, "Exploration of CeO₂ nanoparticles as a chemi-sensor and photo-catalyst for

- environmental applications”, *Sci. Total Environ*, Vol. 409, pp. 2987-2992, 2011.
- [16] M. Darroudi, S. J. Hoseini, R. K. Oskuee, H. A. Hosseini, L. Gholami and Gerayali, *Ceram. Int*, Vol. 40, pp. 7425, 2014.
- [17] K. Sabzevari, H. Adibkia, A. Hashemi, N. Hedayatfar, F. Mohsenzadeh, Atyabi, et.al, “Polymeric triamcinolone acetonide nanoparticles as a new alternative in the treatment of uveitis: In vitro and in vivo studies”, *Eur. J. Pharm. Biopharm*, Vol. 84, pp. 63-71, 2013.
- [18] S. Maensiri, S. Labuayai, J. Laokul, Klinkaewnarong and E. Swatsitang, *Jpn. J. Appl. Phys*, Vol. 53, pp. 06-14, 2014.
- [19] P. Singh and A. Nanda, “Enhanced sun protection of nano-sized metal oxide particles over conventional metal oxide particles: An in vitro comparative study”, *Int. J. Cosmetic Sci*, Vol. 36, pp. 273-283, 2014.
- [20] Y. R. Gao and Cranston, *Textile Research Journal*, Vol. 78, pp. 60-72, 2008.
- [21] S. Neeraj, N. Kijima, and A. K. Cheetham, *Chem. Phys. Lett*, Vol. 387, pp. 2-6, 2004.
- [22] S. Pokhrel and K. S. Nagaraja, *Phy. Stat. Sol. A*, Vol. 343, 2003.

High lights

- Simple method of preparation, non-toxic, using green capping agent.
- Cubic phase of CeO₂ with crystallite size of 29.05 nm.
- Bunches of small spherical like morphology with high porosity, band gap 3.76 eV.
- Highest sensitivity factor $S_f = 2876$.
- Encouraging antibacterial activity against micro-organisms.